The Ultrafast Structural Pathway of Charge Transfer in N, N, N', N'-Tetramethylethylenediamine.

ARTICLE *in* THE JOURNAL OF PHYSICAL CHEMISTRY A · FEBRUARY 2015

Impact Factor: 2.69 · DOI: 10.1021/acs.jpca.5b01797 · Source: PubMed

5 AUTHORS, INCLUDING:

Xinxin Cheng
University of Hamburg
9 PUBLICATIONS **18** CITATIONS
SEE PROFILE

Yao Zhang
Brown University
8 PUBLICATIONS **23** CITATIONS
SEE PROFILE

Yan Gao
Brown University
6 PUBLICATIONS **13** CITATIONS
SEE PROFILE

Hannes Jonsson
University of Iceland
194 PUBLICATIONS **15,215** CITATIONS
SEE PROFILE

THE JOURNAL OF PHYSICAL CHEMISTRY A

Article

pubs.acs.org/JPCA

Ultrafast Structural Pathway of Charge Transfer in *N,N,N′,N′*-Tetramethylethylenediamine

Xinxin Cheng,[†] Yao Zhang,[†] Yan Gao,[†] Hannes Jónsson,[†,‡] and Peter M. Weber*[,†]

[†]Department of Chemistry, Brown University, Providence, Rhode Island 02912, United States

[‡]Faculty of Physical Sciences, VR-III, University of Iceland, 107 Reykjavík, Iceland

ABSTRACT: We have explored the ultrafast molecular structural dynamics associated with charge transfer in *N,N,N′,N′*-tetramethylethylenediamine using Rydberg fingerprint spectroscopy in conjunction with self-interaction corrected density functional theory. Excitation at 239 nm prepares the molecule in the Franck−Condon region of the 3s state with the charge localized on one of the two amine groups. As seen from the time-dependent Rydberg electron binding energies, the pathway of the rapidly ensuing dynamics leads through several structurally distinct conformers with various degrees of charge localization before reaching the fully charge-delocalized structure on a picosecond time scale. At several steps along the reaction path, the transient structures are identified through a comparison of the spectroscopically observed binding energies with computed values. The molecular structure is seen to evolve dynamically from an initially folded conformer to the stretched form that supports charge delocalization before an equilibrium sets in with forward and backward time constants of 1.19 (0.14) and 2.61 (0.31) ps, respectively. A coherent wavepacket motion in the charge-localized state with a period of 270 (17) fs and damping of 430 (260) fs is observed and tentatively assigned to the nitrogen umbrella motion. The damping time constant indicates the rate of the energy flow into other vibrations that are not activated by the optical excitation.

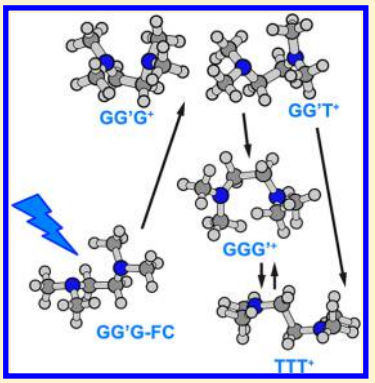

INTRODUCTION

Understanding the nuclear and electron motions during chemical reactions is important for designing novel catalysts, exploring new reaction paths, and selectively controlling reactions on the molecular level. Among the many types of chemical reactions, those involved with charge transfer (CT) are especially important because of their relevance to many reactions in chemical synthesis, to biological systems such as DNA and proteins, and to the mechanistic processes in nanoscale devices.[1−4] To monitor molecular dynamics in real time, pump−probe techniques[2] have been widely used in conjunction with traditional spectroscopic techniques such as absorption spectroscopy, Raman scattering, and photoelectron spectroscopy. With recent progress in the generation of ultrafast pulsed, intense X-ray beams and ultrafast electron sources, time-resolved gas-phase X-ray and electron diffractions also have great potential to directly map molecular structures in real time.[5,6] Despite these advances in determining real-time molecular structures, the observation of structural dynamics at high effective temperature, where chemical reactions often proceed, remains challenging because of the vibrational congestion and structural dispersion. This problem is particularly pertinent for structurally flexible molecules that often arise as intermediates during chemical reactions. Additionally, the large facilities often associated with ultrafast, intense X-ray or electron beams further limit their applications. In contrast, time-resolved Rydberg fingerprint spectroscopy (RFS), in conjunction with variational, self-consistent density functional theory including self-interaction correction (DFT-SIC), has proven its ability to capture the structural dynamics of hot and floppy molecules.[7−9] We have applied this approach to search for structural transients in the charge delocalization dynamics of *N,N,N′,N′*-tetramethylethylenediamine (TMEDA). Dramatic as well as subtle structural changes have been identified revealing a molecular reaction path involving distinct conformeric forms over a subpicosecond time scale.

RFS takes advantage of the sensitivity of the binding energy (BE) of a Rydberg electron to both the structure and the charge distribution of a molecular ion core, coupled with its insensitivity to vibrational excitations.[10−12] Time-resolved measurement of the BE has emerged as an effective tool to probe molecular structural dynamics, such as the hydrogen-transfer process in large molecular clusters,[13] the conformational dynamics in hot flexible aliphatic molecules,[14] and the CT dynamics in a bifunctional molecule,[15] and several systems with multiple ionization centers.[16,17] The molecular ion core of a Rydberg state closely resembles the molecular cation because the distant Rydberg electron has a weak effect on the chemical bonding of the core. Because the ejection of a photoelectron is fast compared to nuclear motions, the photoelectron spectra reflect the molecular structure at the time that the electron is ejected. The structural dynamics is observed by inserting a time delay between the excitation of the molecule and its ionization. To identify specific molecular transients, we compute the BEs

Received: February 23, 2015
Published: February 25, 2015

DOI: 10.1021/acs.jpca.5b01797
J. Phys. Chem. A 2015, 119, 2813−2818

of potential structures using DFT-SIC and compare the computational results to the observed spectra.

TMEDA and its derivatives have previously served as molecular models to investigate electron lone pair interactions and charge delocalization.[18−23] In its ground state, TMEDA has negligible lone pair interaction as evidenced by photoionization and optical electronic absorption spectrosocpy.[17,21,24] A delayed onset of the charge-resonant electronic absorption signal of several aliphatic diamine (including TMEDA) radical cations in rigid matrix environments indicates a structure-dependent intramolecular charge delocalization.[25,26] A recent RFS study[17] showed that a 209 nm photon excites the TMEDA molecule to a 3p Rydberg state with a charge-localized ion core. Rapid internal conversion from 3p to 3s generates a multitude of conformational structures, including one where the nitrogen lone pair orbitals align to enable the charge delocalization between the two nitrogen atoms. Because the internal conversion populates multiple conformeric structures, including some that are close to that of the original ground state, as well as the charge-delocalized structure, the structural details of the charge delocalization reaction have remained hidden in these previous studies. In exploring the dependence of the CT dynamics on the excitation energy, we found that lower-energy pump photons excite TMEDA directly to the 3s Rydberg state, which unmasks the structural motions that lead from the Franck−Condon (FC) region to the charge-delocalized state.

METHODOLOGY

The photoelectron spectroscopy apparatus has been described previously.[27,28] Photoelectrons were detected using microchannel plate detectors, and their flight times were converted to kinetic energies. The BE of an electron in a Rydberg state was determined by subtracting the kinetic energy from the probe photon energy. The laser system has been described.[17] Briefly, the 239 nm pump pulse and the 404 nm probe pulse were generated by an optical parametric amplifier (Coherent Opera SOLO) and BBO upconversion crystals, respectively, with the 808 nm fundamental pulses from a two-stage amplifier (Coherent Legend Elite Duo) at a 5 kHz repetition rate. The laser beams were focused perpendicularly onto the molecular beam, which was generated by entraining TMEDA at −30 °C in a stream of helium carrier gas and expanding through a 100 μm nozzle and a 150 μm skimmer. The time zero of the laser pulse overlap was determined by monitoring the cross-correlation between the pulses using the molecular response of 1,4-dimethylpiperazine, giving a cross-correlation time of 97(2) fs fwhm.

The structures and relative energies (REs) of the ground state and ion state of TMEDA used to calculate the BEs in this work have been reported elsewhere.[17] The BEs of the Rydberg states were calculated using the DFT-SIC method with the Perdew−Zunger self-interaction correction,[29] carried out with the GPAW program[30,31] using a real space grid with a cubic simulation box of 25 Å side length and a uniform grid spacing of 0.15 Å. The Rydberg orbitals were calculated using the ground-state DFT-SIC with the local density approximation (LDA) functional.[32] The total energy of the Rydberg excited state was calculated with the PBE functional[33] and the delta self-consistent field method,[34] where one electron was removed from the highest occupied orbital (HOMO) and placed in the desired Rydberg orbital. The BE of the Rydberg excited state was then obtained by subtracting the total energy of the excited-state energy from that of the ion. This approach has been shown to give good results for both molecules and molecular clusters.[7−9]

RESULTS AND DISCUSSION

The contour plot of the time-resolved Rydberg electron BE spectrum is shown in Figure 1a. The 239 nm (5.19 eV) pump pulse resonantly excites TMEDA to the 3s Rydberg state, and the 404 nm (3.07 eV) probe pulse monitors the time-dependent dynamics by ionizing the Rydberg excited molecules. In analogy to our previous studies of other tertiary amines and the recent RFS study on TMEDA,[17,35,36] we assign the peaks at about 2.84 and 2.69 eV to 3s Rydberg states associated with two distinct molecular structures. We label the two peaks as 3s_h and 3s_l, where h and l denote the higher and lower BE, respectively. Figure 1b shows the energy-integrated intensities of the 3s_h (2.64−2.75 eV) and 3s_l (2.75−2.95 eV). Figure 1c shows their corresponding fractions. In the observed time window, the total intensity of the 3s state does not decay. This compares to a relatively short lifetime (6.77 ps) of the 3s state when the molecule is excited with a higher-energy 209 nm photon. A dependence of electronic state lifetimes on vibrational excitation has previously been documented.[37] In *N*,*N*-dimethylisopropylamine, the lifetime of the 3s Rydberg state decreases exponentially with the amount of vibrational energy. Assuming equal ionization cross sections for the two states and given careful calibration of the intensity sensitivity of the photoelectron spectrometer for electrons with different kinetic energies, the fractional intensity represents the populations of the different structural forms. It is apparent that the 239 nm photon populates the 3s_h state

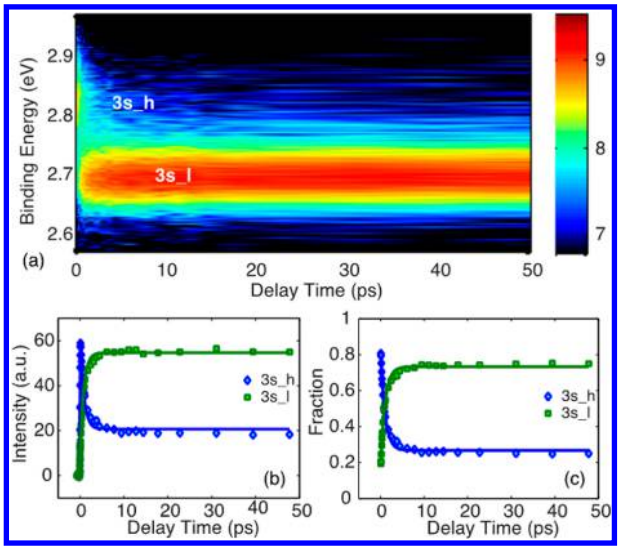

Figure 1. (a) Time-dependent Rydberg electron BE spectrum of TMEDA pumped with 239 nm and probed with 404 nm. The colors represent the signal intensities on a natural logarithmic scale, and the color bar gives the scale range in arbitrary units. 3s_h and 3s_l represent the 3s component peaks with higher and lower BE, respectively. (b) Time-dependent signals of the two spectral features in arbitrary units (3s_h in blue diamonds and 3s_l in green squares). (c) Time-dependent intensity fractions of the 3s_h and 3s_l peaks. Solid lines in (b) and (c) represent the best fits of the experimental data with a kinetics model of first-order reactions and a two-component equilibrium. The values of the fit parameters are discussed in the text.

DOI: 10.1021/acs.jpca.5b01797
J. Phys. Chem. A 2015, 119, 2813−2818

directly, but the flow of energy leads to population of the 3s_l state until an equilibrium is reached.

Assuming first-order kinetics and adopting the formalism of a two-component system that is suddenly displaced from its equilibrium,[14,38] the experimental data on the intensities and the fractional ratios can be fitted as shown by solid lines in Figure 1b and c. The forward and backward time constants of the reaction from 3s_h to 3s_l were determined to be 1.19 (0.14) and 2.61 (0.31) ps, respectively. Values in the parentheses give the 3σ uncertainty of the fits. These time constants are much larger than those measured in experiments where the molecule is pumped with 209 nm,[17] which are 490 (55) and 621 (56) fs for the forward and backward reactions, respectively. The slower equilibrium rates are likely due to the smaller available vibrational energy in the longer pump wavelength experiments and are consistent with longer electronic state lifetimes. Once equilibrium is reached, the population ratios are 0.267 (0.013) and 0.733 (0.013) for the 3s_h and 3s_l peaks, respectively. At time zero, the displacement of the population ratio from the equilibrium value is 0.563 (0.031). In the prior experiments with 209 nm pump photons, the equilibrium population ratios were 0.415 (0.027) and 0.585 (0.027) for the 3s_h and 3s_l peaks, respectively, and the population ratio displacement was 0.269 (0.070). The dependence of the equilibrium population on the wavelength indicates negative enthalpy and entropy changes for the reaction from 3s_h to 3s_l.

To explore the dynamical pathway that leads TMEDA from the FC region to the equilibrium, we honed in on the early time dynamics by increasing the number of delay time steps within the first 2 ps. At short delay times, we discovered several distinct BE peaks in the time-resolved Rydberg electron BE spectrum, indicated by numbers 1−4 in Figure 2a. At time zero, the 3s_h peak arises first in position 1, while the 3s_l peak has negligible intensity at that time. As time passes, the 3s_h peak center migrates toward higher BEs, reaching position 2 at 0.6 ps. It then moves back toward a lower BE, position 3, and becomes constant after about 1 ps. During this entire process, the 3s_l peak retains a constant BE. We interpret this observation as reflecting structural dynamics among distinct conformers, superimposed on the overall approach to the equilibrium distribution.

To obtain the center positions of the discrete peaks, we fitted the spectra at each time point with one Lorentzian function in the time range of 0−0.23 ps and two Lorentzian components thereafter. This yields the time-dependent peak center positions of the 3s_h and 3s_l peaks as shown in Figure 2b. The solid lines in light blue and light green show the best fits of the equilibrium peak center positions of the 3s_h and 3s_l peaks, respectively, after they have settled to constant values. The peak positions are listed in Table 1.

To assign the observed spectroscopic features to molecular structures, we calculated the BEs for the known minimum-energy structures of the ground state and the ion state.[17] TMEDA conformers are labeled with G or gauche, T or trans, and G′ or gauche′, meaning that the dihedral angle D(LP−N−C−C) or D(N−C−C−N) is in the range of 0−120°, 120−240°, and 240−360 or −120−0°, respectively. LP stands for the electron lone pair of the N atom. The folded GG′G structure is the global minimum in the ground state and is the one present in the molecular beam. In the cation, the three most stable conformers are TTT^+, GGG'^+, and $GG'G^+$. The fully stretched TTT^+ conformer was found to be the global minimum in the

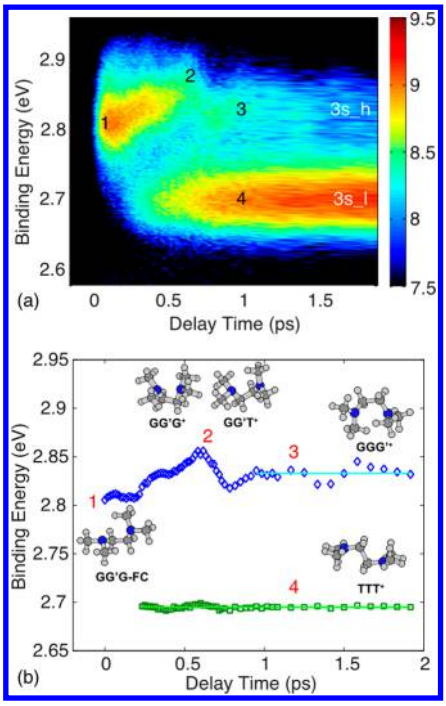

Figure 2. (a) The early part of the time-dependent Rydberg electron BE spectrum, with four distinct peak positions labeled by numbers 1−4, in the 3s_h and 3s_l regions. (b) The peak centers of the deconvoluted 3s peak with a higher BE (3s_h, blue diamonds and line) and a lower BE (3s_l, green squares and line). Numbers 1−4 indicate the same four positions as those in part (a).

Table 1. Experimental BE Peak Center Positions and the Calculated BEs and REs of the 3s Rydberg States[a]

	experimental	calculated		
peak	BE/eV	BE/eV	RE/eV	structures
1	2.81 (1)	2.79	0.85	GG′G-FC
2	2.86 (1)	2.88	0.40	$GG'T^+$
		2.88	0.25	$GG'G^+$
3	2.83 (1)	2.85	0.045	GGG'^+
4	2.70 (1)	2.71	0	TTT^+

[a]The values in parentheses show the 1σ uncertainty in the last digit.

cationic ground state. Starting the optimization on the ion potential surface with the ground-state global minimum GG′G conformer gave the $GG'G^+$ structure. The charge-localized $GG'T^+$ structure was obtained by optimizing the GG′G conformer with one nitrogen semiplanar as the starting structure on the ion potential surface.

For each of these cationic structures, we calculated the BEs using the DFT-SIC method. We assume here that the Rydberg electron has a negligible effect on the structure of the molecular ion core so that the cationic structures resemble those of the corresponding ion cores of the Rydberg excited molecules. Because nuclear motions are much slower than those of the electrons, the molecule should retain its ground-state structure at short delay times. We therefore also calculated the BE of the GG′G structure in the FC region. The calculated BEs and REs of the 3s Rydberg states are listed in Table 1.

The calculated BEs are in excellent agreement with the experimental observations for the given assignments. In the FC region, the molecule retains the ground-state structure GG′G, for which the calculated BE, 2.79 eV, matches well with the

DOI: 10.1021/acs.jpca.5b01797
J. Phys. Chem. A 2015, 119, 2813−2818

experimental value of 2.81(1) eV. Because the FC structure is unstable and has high energy (0.85 eV) on the potential surface of the 3s Rydberg state, the structure of the TMEDA molecule evolves toward a nearby minimum. Because of the negligible interaction of the electron lone pairs in the ground-state structure, the optical excitation leads to a 3s Rydberg state with the charge center at one of the nitrogen atoms, which becomes planar upon excitation. Optimization from the ground-state structure GG′G on the ion surface with different initial conditions yields, as previously pointed out,[17] the $GG'G^+$ and $GG'T^+$ structures. The $GG'G^+$ conformer shows a through-space interaction (TSI) and partial charge delocalization between the two nitrogen atoms, while the $GG'T^+$ conformer has the charge localized on one nitrogen atom.[17,18] The calculated BEs of the $GG'G^+$ and $GG'T^+$ structures are both 2.88 eV, which agrees well with the experimental value of 2.86(1) eV. The continuously increasing BE from peak position 1 to 2 reveals the structural dynamics of the TMEDA ion core upon excitation to the Rydberg state. The structural change mainly involves the nitrogen umbrella motion and a minor internal rotation (D(LP−N−C−C) and D(N−C−C−N)). These motions are probably coupled, and all contribute to the BE change. The $GG'G^+$ and $GG'T^+$ structures therefore both contribute to the peak intensity at 2.86(1) eV.

The two most stable conformers GGG'^+ and TTT^+ both have through-bond interaction (TBI) and a complete charge delocalization over the two nitrogen atoms.[17,18] Reaching these structures from the FC structure requires substantial internal rotation, that is, large changes of the D(N−C−C−N) and the two D(LP−N−C−C) dihedral angles. This means that the TMEDA molecule needs to sample the multidimensional potential surface until it finds the proper geometry where the two lone pairs have strong TBI and the charge can delocalize. The BEs calculated with the GGG'^+ and TTT^+ structures are 2.85 and 2.71 eV, respectively. Therefore, peak position 3 with a 2.83(1) eV BE is assigned to the 3s Rydberg state with the GGG'^+ structure, and peak position 4 with a 2.70(1) eV BE is assigned to 3s with the TTT^+ structure. While initially these two states are at nonequilibrium populations, they continue to convert into each other until an equilibrium is reached. Because the 3s_l peak dominates the intensity at long delay times (Figure 1), the assignment is also consistent with the equilibrium composition where the TTT^+ structure has the lowest total energy (Table 1).

On the basis of these assignments, the structural evolution associated with the CT can be identified. Excitation from the ground state to the 3s Rydberg state initially places a positive charge on only one of the nitrogen atoms and creates a charge-localized state. However, the FC geometry is not a favorable one; therefore, the molecule relaxes to lower its potential energy, resulting in a structural change that is observed as a shift of the BE toward higher values. One of the relaxed structures, $GG'G^+$, exhibits TSI and a delocalized charge character, while another, the $GG'T^+$ conformer, has a localized charge. The molecule has sufficient internal energy to continue to sample the potential surface and find the GGG'^+ and TTT^+ geometries, which have TBI and completely delocalized charges. As the TTT^+ conformer gains in population, the back reaction sets in, which, on a picosecond time scale, leads to a kinetic equilibrium that is dominated by GGG'^+ and TTT^+. The forward and backward time constants of the reaction from 3s_h to 3s_l are 1.19 (0.14) and 2.61 (0.31) ps, respectively.

We note that superimposed on the steady BE increase there are three oscillations during the first 600 fs of the time evolution (Figure 2b). To extract the dynamical information, we first fit the BE center position to a line, as shown in Figure 3. This shows that the BE increases with a rate of 84 (11) meV/ps. The pure oscillation is obtained by subtracting the linear fit from the experimental data, as shown in the inset of Figure 3. Fitting the oscillation to a damped sinusoidal function gives a period of 270 (17) fs with a 430 (260) fs damping factor. The values in parentheses are the 3σ uncertainty. The oscillations are likely due to structural oscillations related to the nitrogen umbrella motion that is induced by the initial excitation. These periodic motions are captured as a BE change as the structure evolves. The damping indicates the flow of energy into vibrations other than the one initially activated. Because the transient structures involved are not minima on the potential surface, they are not reproduced by the current calculation with equilibrium structures. Their existence, however, is clearly indicated by the time-resolved RFS.

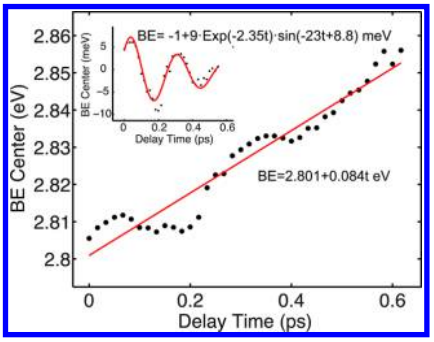

Figure 3. Increase of the BE and superimposed oscillations. Black dots are the experimental data. Red lines show a best fit of the linear dependence and of the oscillatory residual to a damped harmonic oscillation.

CONCLUSIONS

The present study of TMEDA shows the capability of time-resolved RFS to probe the structural dynamics of molecules with large vibrational energy. The large size of the 3s Rydberg orbital and the sensitivity of its BE on the molecular structure make RFS a powerful tool to probe structure-dependent interactions, such as CT reactions, in large molecules. As presented here, the structural pathway and the initial coherent wavepacket motion and energy redistribution are revealed by the RFS in the form of changes of the BE center and amplitude. The ability of the DFT-SIC method to accurately estimate the BEs is essential to positively identify the molecular structures from the observed spectroscopic features. While these computations can explain the major features of the spectra, the BEs can, at the present time, only be applied to sample metastable structures. The experimental RFS, however, has richer dynamical information as it covers the complete evolution of the molecular structure, including structures outside of the minima on the potential energy surface. Future BE and trajectory calculations on the 3s Rydberg surface might resolve in even more clarity the structural changes that occur when the charge delocalizes in TMEDA.

DOI: 10.1021/acs.jpca.5b01797
J. Phys. Chem. A 2015, 119, 2813−2818

AUTHOR INFORMATION

Corresponding Author

*E-mail: peter_weber@brown.edu. Fax: +1-401-863-2594.

Notes

The authors declare no competing financial interest.

ACKNOWLEDGMENTS

This project was supported in part by DTRA, Grant No. HDTRA1-14-1-0008, and by the Icelandic Research Fund. The simulation and energy calculations of the molecular structures were conducted using computational resources and services at the Center for Computation and Visualization, Brown University.

ABBREVIATIONS

CT, charge transfer; RSF, Rydberg fingerprint spectroscopy; DFT-SIC, density functional theory including self-interaction correction; TMEDA, *N,N,N′,N′*-tetramethylethylenediamine; BE, binding energy; RE, relative energy; FC, Franck−Condon; TSI, through-space interaction; TBI, through-bond interaction

REFERENCES

(1) Wan, C. Z.; Fiebig, T.; Schiemann, O.; Barton, J. K.; Zewail, A. H. Femtosecond direct observation of charge transfer between bases in DNA. *Proc. Natl. Acad. Sci. U.S.A.* **2000**, *97*, 14052−14055.

(2) Zewail, A. H. Femtochemistry: Atomic-scale dynamics of the chemical bond using ultrafast lasers (Nobel lecture). *Angew. Chem., Int. Ed.* **2000**, *39*, 2587−2631.

(3) Wasielewski, M. R. Energy, charge, and spin transport in molecules and self-assembled nanostructures inspired by photosynthesis. *J. Org. Chem.* **2006**, *71*, 5051−66.

(4) Moser, C. C.; Keske, J. M.; Warncke, K.; Farid, R. S.; Dutton, P. L. Nature of biological electron transfer. *Nature* **1992**, *355*, 796−802.

(5) Chergui, M.; Zewail, A. H. Electron and X-ray methods of ultrafast structural dynamics: Advances and applications. *ChemPhysChem* **2009**, *10*, 28−43.

(6) Miller, R. J. D. Mapping Atomic Motions with Ultrabright Electrons: The Chemists' Gedanken Experiment Enters the Lab Frame. *Annu. Rev. Phys. Chem.* **2014**, *65*, 583−604.

(7) Gudmundsdóttir, H.; Zhang, Y.; Weber, P. M.; Jónsson, H. Self-interaction corrected density functional calculations of molecular Rydberg states. *J. Chem. Phys.* **2013**, *139*, 194102.

(8) Gudmundsdóttir, H.; Zhang, Y.; Weber, P. M.; Jónsson, H. Self-interaction corrected density functional calculations of Rydberg states of molecular clusters: N,N-dimethylisopropylamine. *J. Chem. Phys.* **2014**, *141*, 234308.

(9) Lehtola, S.; Jónsson, H. Variational, Self-Consistent Implementation of the Perdew−Zunger Self-Interaction Correction with Complex Optimal Orbitals. *J. Chem. Theory Comput.* **2014**, *10*, 5324−5337.

(10) Kuthirummal, N.; Weber, P. M. Rydberg states: Sensitive probes of molecular structure. *Chem. Phys. Lett.* **2003**, *378*, 647−653.

(11) Gosselin, J. L.; Weber, P. M. Rydberg fingerprint spectroscopy: A new spectroscopic tool with local and global structural sensitivity. *J. Phys. Chem. A* **2005**, *109*, 4899−904.

(12) Kuthirummal, N.; Weber, P. M. Structure sensitive photoionization via Rydberg levels. *J. Mol. Struct.* **2006**, *787*, 163−166.

(13) Deb, S.; Minitti, M. P.; Weber, P. M. Structural dynamics and energy flow in Rydberg-excited clusters of N,N-dimethylisopropylamine. *J. Chem. Phys.* **2011**, *135*, 044319.

(14) Minitti, M. P.; Weber, P. M. Time-resolved conformational dynamics in hydrocarbon chains. *Phys. Rev. Lett.* **2007**, *98*, 253004.

(15) Bush, J. C.; Minitti, M. P.; Weber, P. M. Dissociative energy flow, vibrational energy redistribution, and conformeric structural dynamics in bifunctional amine model systems. *J. Phys. Chem. A* **2010**, *114*, 11078−84.

(16) Deb, S.; Cheng, X.; Weber, P. M. Structural Dynamics and Charge Transfer in Electronically Excited *N,N′*-Dimethylpiperazine. *J. Phys. Chem. Lett.* **2013**, *4*, 2780−2784.

(17) Cheng, X.; Zhang, Y.; Deb, S.; Minitti, M. P.; Gao, Y.; Jónsson, H.; Weber, P. M. Ultrafast structural dynamics in Rydberg excited N,N,N′,N′-tetramethylethylenediamine: Conformation dependent electron lone pair interaction and charge delocalization. *Chem. Sci.* **2014**, *5*, 4394−4403.

(18) Hoffmann, R. Interaction of Orbitals through Space and through Bonds. *Acc. Chem. Res.* **1971**, *4*, 1−9.

(19) Heilbronner, E.; Muszkat, K. A. On the Relative Importance of Through-Space vs Through-Bond Interaction between the Lone Pairs in 1,4-Diazabicyclo[2.2.2]octanel. *J. Am. Chem. Soc.* **1970**, *2*, 3818−3821.

(20) Nelsen, S. F.; Buschek, J. M. Photoelectron-Spectra of Some Cyclic Diamines and Polyamines — Lone Pair−Lone Pair Interaction in 1,3-Diamines and 1,4-Diamines. *J. Am. Chem. Soc.* **1974**, *96*, 7930−7934.

(21) Halpern, A. M.; Gartman, T. Structural Effects on Photophysical Processes in Saturated Amines. 2. *J. Am. Chem. Soc.* **1974**, *96*, 1393−1398.

(22) Alder, R. W.; Arrowsmith, R. J.; Casson, A.; Sessions, R. B.; Heilbronner, E.; Kovac, B.; Huber, H.; Taagepera, M. Proton Affinities and Ionization Energies of Bicyclic Amines and Diamines, The Effects of Ring Strain and of 3-Electron σ Bonding. *J. Am. Chem. Soc.* **1981**, *103*, 6137−6142.

(23) Brouwer, A. M.; Zwier, J. M.; Svendsen, C.; Mortensen, O. S.; Langkilde, F. W.; Wilbrandt, R. Radical cation of *N,N*-Dimethylpiperazine: Dramatic structural effects of orbital interactions through bonds. *J. Am. Chem. Soc.* **1998**, *120*, 3748−3757.

(24) Halpern, A. M.; Roebber, J. L.; Weiss, K. Electronic Structure of Cage Amines — Absorption Spectra of Triethylenediamine and Quinuclidine. *J. Chem. Phys.* **1968**, *49*, 1348−1357.

(25) Marcinek, A.; Gebicki, J.; Plonka, A. Microenvironmental Effects in Solid-State Reactions — Dispersive Kinetics of Conformation-Dependent Charge Delocalization in Aliphatic Diamine Radical Cations. *J. Phys. Org. Chem.* **1990**, *3*, 757−759.

(26) Gebicki, J.; Marcinek, A.; Stradowski, C. Electronic Absorption-Spectra of Aliphatic Diamine Radical Cations — Conformation-Dependent Charge Delocalization. *J. Phys. Org. Chem.* **1990**, *3*, 606−610.

(27) Kim, B. J.; Thantu, N.; Weber, P. M. High-Resolution Photoelectron-Spectroscopy — The Vibrational-Spectrum of the 2-Aminopyridine Cation. *J. Chem. Phys.* **1992**, *97*, 5384−5391.

(28) Cheng, W.; Kuthirummal, N.; Gosselin, J. L.; Solling, T. I.; Weinkauf, R.; Weber, P. M. Control of local ionization and charge transfer in the bifunctional molecule 2-phenylethyl-*N,N*-dimethylamine using Rydberg fingerprint spectroscopy. *J. Phys. Chem. A* **2005**, *109*, 1920−5.

(29) Perdew, J. P.; Zunger, A. Self-Interaction Correction to Density-Functional Approximations for Many-Electron Systems. *Phys. Rev. B* **1981**, *23*, 5048−5079.

(30) Mortensen, J. J.; Hansen, L. B.; Jacobsen, K. W. Real-space grid implementation of the projector augmented wave method. *Phys. Rev. B* **2005**, *71*, 035109.

(31) Enkovaara, J.; Rostgaard, C.; Mortensen, J. J.; Chen, J.; Dulak, M.; Ferrighi, L.; Gavnholt, J.; Glinsvad, C.; Haikola, V.; Hansen, H. A.; Kristoffersen, H. H.; Kuisma, M.; Larsen, A. H.; Lehtovaara, L.; Ljungberg, M.; Lopez-Acevedo, O.; Moses, P. G.; Ojanen, J.; Olsen, T.; Petzold, V.; Romero, N. A.; Stausholm-Møller, J.; Strange, M.; Tritsaris, G. A.; Vanin, M.; Walter, M.; Hammer, B.; Hakkinen, H.; Madsen, G. K.; Nieminen, R. M.; Nørskov, J. K.; Puska, M.; Rantala, T. T.; Schiøtz, J.; Thygesen, K. S.; Jacobsen, K. W. Electronic structure calculations with GPAW: a real-space implementation of the projector augmented-wave method. *J. Phys.: Condens. Matter* **2010**, *22*, 253202.

(32) Kohn, W.; Sham, L. J. Self-Consistent Equations Including Exchange and Correlation Effects. *Phys. Rev.* **1965**, *140*, 1133.

(33) Perdew, J. P.; Burke, K.; Ernzerhof, M. Generalized gradient approximation made simple. *Phys. Rev. Lett.* **1996**, *77*, 3865−3868.

DOI: 10.1021/acs.jpca.5b01797
J. Phys. Chem. A 2015, 119, 2813−2818

(34) Gavnholt, J.; Olsen, T.; Engelund, M.; Schiøtz, J. Delta self-consistent field method to obtain potential energy surfaces of excited molecules on surfaces. *Phys. Rev. B* **2008**, *78*, 075441.
(35) Minitti, M. P.; Cardoza, J. D.; Weber, P. M. Rydberg fingerprint spectroscopy of hot molecules: Structural dispersion in flexible hydrocarbons. *J. Phys. Chem. A* **2006**, *110*, 10212−8.
(36) Gosselin, J. L.; Minitti, M. P.; Rudakov, F. M.; Solling, T. I.; Weber, P. M. Energy flow and fragmentation dynamics of *N*,*N*-dimethylisopropylamine. *J. Phys. Chem. A* **2006**, *110*, 4251−5.
(37) Rudakov, F.; Zhang, Y.; Cheng, X.; Weber, P. M. Standoff trace chemical sensing via manipulation of excited electronic state lifetimes. *Opt. Lett.* **2013**, *38*, 4445−8.
(38) Houston, P.L. *Chemical Kinetics and Reaction Dynamics*; McGraw-Hill: New York, 2001.

DOI: 10.1021/acs.jpca.5b01797
J. Phys. Chem. A 2015, 119, 2813−2818